JCTC Journal of Chemical Theory and Computation

Article

pubs.acs.org/JCTC

Trivalent Uranium Complex As a Catalyst to Promote the Functionalization of Carbon Dioxide and Carbon Disulfide: A Computational Mechanistic Study

Wanjian Ding,[†,*] Weihai Fang,[†] Zhifang Chai,[‡] and Dongqi Wang[‡,*]

[†]College of Chemistry, Beijing Normal University, Beijing, 100875, P. R. China

[‡]Laboratory of Nuclear Analysis Techniques, Institute of High Energy Physics, Chinese Academy of Sciences, Beijing, 100049, P. R. China

Supporting Information

ABSTRACT: We report our recent DFT mechanistic study on the functionalization of CO_2 and CS_2 promoted by a trivalent uranium complex $(Tp^*)_2UCH_2Ph$. In the calculations, the uranium atom is described by a quasi-relativistic 5f-in-core ECP basis set (LPP) developed for the trivalent uranium cation, which was qualified by the calculations with a quasi-relativistic small core ECP basis set (SPP) for uranium. According to our calculations, the functionalization proceeds in a stepwise manner, and the CO_2 or CS_2 does not interact with the central uranium atom to form a stable complex prior to the reaction due to the steric hindrance from the bulky ligands but directly cleaves the U−C (benzyl) bond by forming a C−C covalent bond. The released coordination site of uranium is concomitantly occupied by one chalcogen atom of the incoming molecule and gives an intermediate with the uranium atom interacting with the functionalized CO_2 or CS_2 in an η^1 fasion. This step is followed by a reorientation of the (dithio)carboxylate side chain of the newly formed $PhCH_2CE_2^-$ (E = O, S) ligand to give the corresponding product. Energetically, the first step is characterized as the rate-determining step with a barrier of 9.5 (CO_2) or 25.0 (CS_2) kcal/mol, and during the reaction, the chalcogen atoms are reduced, while the methylene of the benzyl group is oxidized. Comparison of the results from SPP and LPP calculations indicates that our calculations qualify the use of an LPP treatment of the uranium atom toward a reasonable description of the model systems in the present study.

INTRODUCTION

Due to the unique properties of actinoids arising from the participation of 5f orbitals in its bonding interaction, the application of actinoid molecular systems in homogeneous catalysis is an attractive issue toward the activation of strong bonds that are believed to be extremely stable under ambient conditions. Available work has covered a broad area, among which is the activation of inert small molecules,[1,2] such as CO_2 and CS_2.[2−6] One of the early endeavors relevant to the functionalization of carbon dioxide contributed to the formation of bridged sulfido species, $[\{(\eta^5\text{-}C_5H_4Me)_3U\}_2(\mu\text{-}S)]$, from COS promoted by a trivalent uranium metallocene, $[(\eta^5\text{-}C_5H_4Me)_3U(THF)]$, and the reaction is a two-electron reduction process.[7]

The functionalization of CO_2 and CS_2 is important in the sense of the recycling of such compounds toward the production of chemicals that are currently mainly obtained from petrochemicals, and it opens a new passage toward a carbon economy. However, though being an attractive participator in C1 chemistry, only a few applications have been developed and industrialized, suggesting that the functionalization of CO_2 and CS_2 is challenging and the searching of efficient catalysts calls for the accumulation of more knowledge for a better understanding to guide new development. Studies on this issue cover the formation of new C−O and C−N bonds without reduction of CO_2 ("horizontal approach");[8−11] CO_2 reduction with electrochemical, photoelectrochemical, and chemical methods to formic acid, formaldehyde, and methanol ("vertical approach");[12−20] and the combination of the reduction of CO_2 and the formation of new C−C, C−N, and C−O bonds ("diagonal approach").[21] In these approaches, molecular organometallic systems containing d transition metal have been often considered as catalysts to activate the central C atom,[11] including, but not limited to, iron,[16] iridium,[14,19] niobium,[17,22,23] palladium,[24] rhodium,[25] copper,[26,27] nickel,[13,28,29] vanadium,[23] and samarium.[30−32] The advance in this field has been reviewed.[8,11,12,20,33]

As an extremely stable species, CO_2 is found to be able to coordinate to a metal atom in multiple modes depending on the ligands attached to the metal, and examples are an η^1 fashion of binding mode through carbon in $[(Cy_3P)_2Ni(CO_2)]$ (Cy = cyclohexyl)[34,35] and η^2-COO in $[(diars)_2M(CO_2)(Cl)]$ [diars = *o*-phenylenebis(dimethylarsine); M = Ir, Rh].[36] The binding mode of CO_2 to actinoids (An) is not well recognized,[37] and in a recent study,[38] the η^1 fashion of binding mode through oxygen in $[((^{Ad}ArO)_3tacn)U(CO_2^{\bullet-})]$ was reported, and the complex has been proposed to exist as a charge-separated $[U^{IV}-L^{\bullet-}]$ species, which is a plausible explanation concerning the highly reducing nature of uranium(IV).

With respect to the use of actinoids in the functionalization of CO_2 and CS_2, available work has investigated the uranium molecular systems in its +4 oxidation state.[3,39−44] These studies demonstrated that the insertion of CO_2 may happen in the U(IV)−N[3,39] and U(IV)−S[42] bonds and the insertion of CS_2

Special Issue: Wilfred F. van Gunsteren Festschrift

Received: January 31, 2012
Published: August 7, 2012

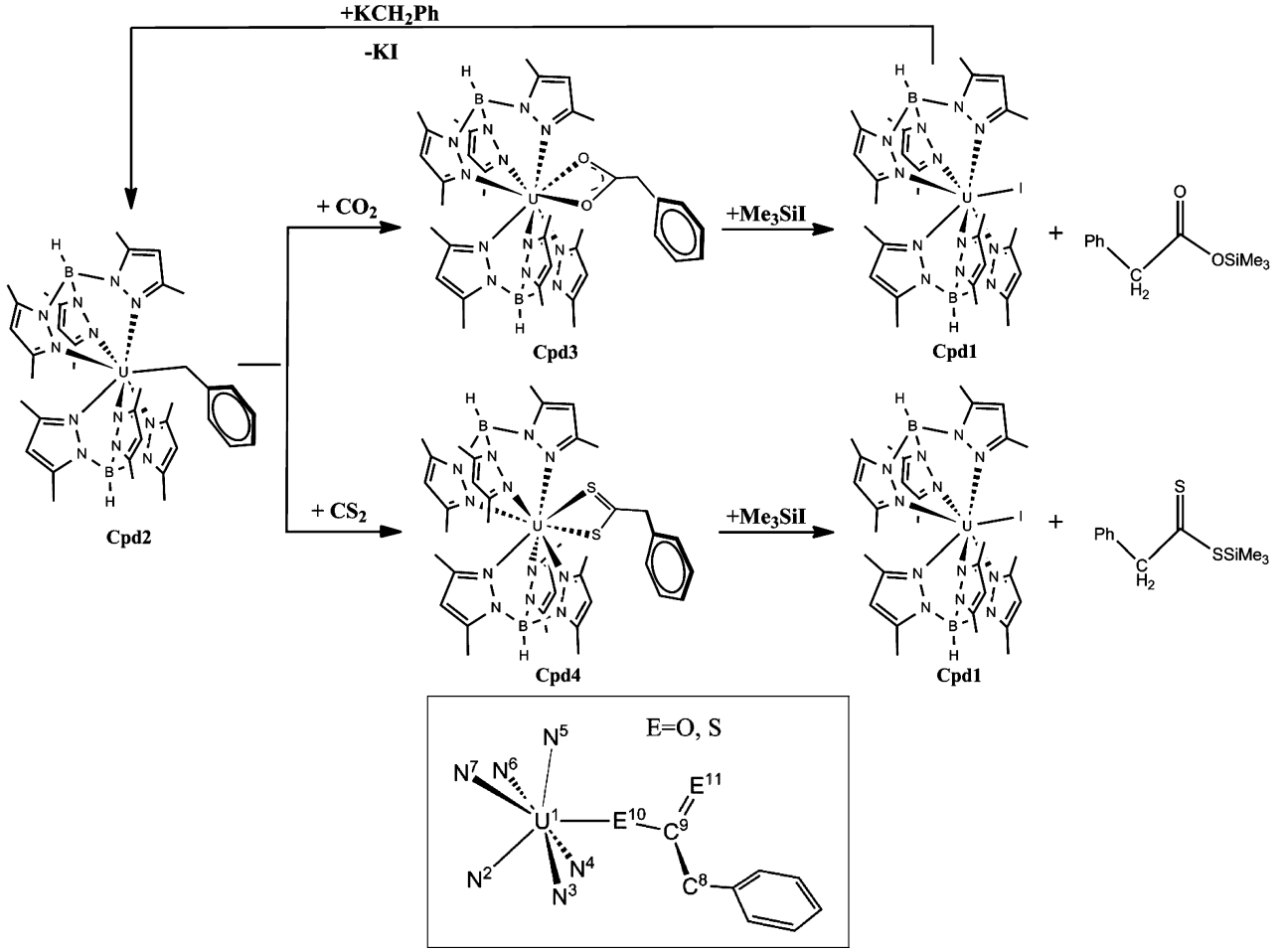

Figure 1. A schematic elucidation of the functionalization of CO_2 and CS_2 and the numbering of key atoms (U, O/S, C_{CO_2}, and C_{benzyl}).

into the U(IV)−N[40] and U(IV)−S[42] bonds. It has also shown the insertion of CO_2 into the U(IV)−C bond,[41,43,44] while this is proved to be difficult for CS_2 given the lack of available data.

Trivalent uranium(III), with an electronic configuration of $[Rn]5f^3$, has also found use in the functionalization of CO_2 and CS_2.[6] The stable form of U(III)−alkyl species is believed to be difficult to isolate due to their strong propensity toward disproportionation.[45] A remediation is the coordination of U(III) with macrocyclic ligands,[6,46] such as bis(hydrotris(3,5-dimethylpyrazolyl)-borate ligand (Tp*), which is a bulky Lewis base and has been shown to be able to stabilize low-valent uranium species.[47,48] These types of stable complexes are potential one-electron reducing agents and may coordinate with small molecules which are to be activated.

Recently, Bart and co-workers[6] reported a new trivalent U(III) complex in which the U(III) is stabilized by Tp*. This complex may exist in the form of salt with an iodide anion and shows reactivity with KCH_2Ph to produce an alkyl complex $(Tp^*)_2UCH_2Ph$ (denoted as Cpd2) through salt metathesis, which can then be used in the functionalization of small compounds such as CO_2 and CS_2[6] but not acetone.[49] For the insertion reaction of CO_2 and CS_2,[6] the intermediate Cpd2 and products ($(Tp^*)_2U$-κ^2-O_2CCH_2Ph and $(Tp^*)_2U$-κ^2-S_2CCH_2Ph, denoted as Cpd3 and Cpd4, respectively) have been isolated (Figure 1). However, the mechanisms that the reactions follow and the activity of the U−S bond remain unknown.[6] These open questions motivated us to carry out a density functional theory mechanistic study on the prototype molecular systems in the experimental work[6] to understand the nature of the functionalization of the CO_2 and CS_2 promoted by a trivalent uranium complex.

COMPUTATIONAL DETAILS

The prototype models in the experimental study[6] were used in the present calculations. For the method, we used the B3PW91 functional,[50,51] in combination with two levels of basis sets, differing in the treatment of the uranium atom by a quasi-relativistic large core (with 81 core electrons and a contraction scheme (7s6p5d)/[4s3p3d] for the valence orbitals)[52] and a quasi-relativistic small core (with 60 core electrons and a contraction scheme (14s13p10d8f6g)/[10s9p5d4f3g] for the valence orbitals)[53−55] ECP together with the corresponding valence basis sets. The other atoms were described by a double-ζ quality basis set, with polarization functions for non-hydrogen atoms, 6-31G(d), except for the iodine atom which is treated by SDD ECP[56] for core shells, together with a description of the valence shell by SDD[56] [SDD(SDD)] or augmented VTZ[57] [SDD(aVTZ)], or by LanL2DZ ECP[58−60] together with the corresponding valence basis set [LanL2DZ(LanL2DZ)]. The combinations of basis sets, depending on the treatment of uranium, are denoted as LPP (5f-in-core large core treatment) and SPP (small core treatment), respectively. In the LPP calculations, the unpaired f electrons were described with pseudopotentials; thus, all of the model systems have closed valence shells and were treated as singlet.

We note that in an earlier study[61] a proper treatment of 5f electrons has been emphasized for a reliable description of the interactions between An(III) and ligands, and a small core treatment shows better performance than a large core treatment. In another work toward the characterization of the role of 5f electrons in organoactinoid reactivity,[62] the 5f electrons were found to be not active in reactions, and a large core treatment of the actinoid atom may give a qualitatively correct description of the reactions when an organoactinoid was involved. The result may be further improved with the inclusion of core-polarization potentials (CPP). In a recent characterization of two U(IV) molecular systems, an SPP treatment of the U atom was used by Bart et al.[63] In order to validate the use of a large core treatment for trivalent uranium in the model systems of functionalization of small molecules, we have subjected the calculations to both LPP and SPP treatments. Note that in the present study we have neglected the contribution of spin−orbit coupling since this work aims at the mechanisms that the functionalization of CO_2 and CS_2 follows and mainly concerns the thermodynamics of the reactions. In those studies toward a precise characterization of electronic properties of a molecular system containing unpaired f electrons, this approximation may become invalid, and a proper treatment of spin−orbit coupling is necessary.

The current investigation covers the issues of the functionalization of CO_2 and CS_2 starting from Cpd2, the consumption of Cpd3 and Cpd4 with the presence of trimethylsilyl iodide (TMSI), and the uncatalyzed reaction of phenyl (dithio)acetic acid with TMSI. To evaluate the influence of the solvent effect of tetrahydrofuran (THF), a polarizable continuum model (PCM)[64] was used for uncatalyzed reactions to reoptimize the stationary points. All of these calculations were done with the B3PW91 functional, except for the functionalization of CO_2 and CS_2, which has been studied with both B3PW91 and TPSS methods to check the consistency of the two functionals in describing the trivalent uranium molecular system. Prior to these calculations, in order to determine the spin states of Cpd2, Cpd3, and Cpd4 at their ground state, i.e., either doublet or quartet, besides the B3PW91 functional, we have also used the BP86,[65,66] TPSS,[67] PBE,[68,69] B3LYP,[50,70] and BHandHLYP[50,70] methods for comparison.

All stationary points reported here have been fully optimized, followed by a vibrational frequency analysis to confirm its nature as either a minimum or a transition state. Intrinsic reaction coordinate (IRC) calculations[71,72] were then carried out for the key steps of a reaction to verify the two minima of a transition state connected.

The program Gaussian 09[73] was employed to carry out the calculations. When calculating the energy profiles of each process, we did not use the B3PW91-optimized reactant complex (RC) as the reference point concerning the deficiency of B3PW91 in describing weak intramolecular interactions, which may become a source of error against a reasonable description of the reaction energetics, but did use the sum of the energies of the separated reactants (RS). All data reported here are from calculations with an SPP treatment for uranium unless stated otherwise.

RESULTS AND DISCUSSIONS

A. SPP vs LPP in the Characterization of Cpd2, Cpd3, and Cpd4. In Cpd2, as seen in Figure 2, the uranium atom is coordinated to two bulky Tp* ligands and a benzyl group, with a coordination number of 7, and has a formal charge of +3 and an electronic configuration of $[Rn]5f^3$, leading to a spin multiplicity of 2 or 4.

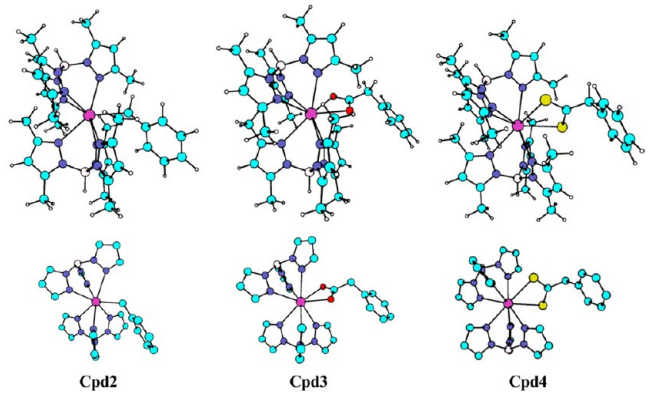

Figure 2. The 3D structures of the three compounds Cpd2, Cpd3, and Cpd4. The second row shows key atoms of the three compounds which are orientated in a way that one can judge the symmetric coordination of the two Tp* ligands to the U atom. Atomic color scheme: C in *cyan*, H in *white*, B in *light pink*, N in *blue*, U in *magenta*, O in *red*, and S in *goldenrod*.

To verify the electronic state in which the reaction proceeds, we have first optimized the three compounds, Cpd2, Cpd3, and Cpd4, in both their doublet and quartet states. The calculations started from the X-ray coordinates of the three compounds,[6] and the relative energies and free energies are tabulated in Table 1. According to the calculated relative electronic energies and free energies, the quartet state is more stable than the doublet state on an order of 10 kcal/mol for all three compounds with different functionals, including BP86,[65,66] TPSS,[67] PBE,[68,69] B3LYP,[50,70] BHandHLYP,[50,70] and B3PW91;[50,51] thus, the ground state is characterized as quartet.

The natural bond orbital (NBO)[74] analysis of the complexes in their quartet states with the B3PW91 functional gives an electronic configuration of $[Rn]7s^{0.2}5f^{3.2}6d^{0.8}7p^{0.2}$ for Cpd2, $[Rn]7s^{0.2}5f^{3.2}6d^{0.8}7p^{0.3}$ for Cpd3, and $[Rn]7s^{0.3}5f^{3.2}6d^{1.1}7p^{0.4}$ for Cpd4 and suggests that in the trivalent uranium complexes under study, the three unpaired electrons prefer to occupy distinct 5f orbitals. The fractional occupations larger than 3 in 5f orbitals suggest that the 5f orbitals may contribute to the metal−ligand (M−L) interactions through back-donation from the ligands. However, the occupations in 5f orbitals do not fluctuate significantly when going from Cpd2 to Cpd3 or to Cpd4, indicating that the contribution of 5f orbitals may be comparable in these three compounds, which provides us confidence in using a 5f-in-core treatment (LPP) of uranium. The recently developed LPP[52] allows a partial occupation in the 5f orbitals to adapt to the situation where 5f orbitals may participate in chemical bonding interactions. According to our calculations (Table 2), LPP gives similar atomic charges of key atoms and descriptions of the bond strength to SPP in view of the Mayer bond order (MBO).[75]

The examination of the reaction systems shows that during the reaction, though the coordination number of the central uranium may change, it does not interact with strong field ligands; thus, we do not expect a significant impact from the electrons in the inner shells. To confirm this, we have also monitored the fluctuation of atomic partial charge and spin densities along the reactions (Figure 5), which will be discussed in a later part of this paper.

Besides the consistent results of the population analysis in the LPP and SPP calculations, they also give almost identical relative energies for the reactions

$$Cpd2 + CO_2 \rightarrow Cpd3 \quad (1)$$

$$Cpd2 + CS_2 \rightarrow Cpd4 \quad (2)$$

Table 1. Zero-Point Energy Corrected Relative Energies (kcal/mol) between Quartet (E^q) and Doublet (E^d) States of Cpd2, Cpd3, and Cpd4 from SPP Calculations,[a] $\langle S^2\rangle$ (Doublet/Quartet), and the Reaction Energies (kcal/mol) for the Formation of Cpd3 and Cpd4 in Their Quartet States from SPP and LPP Calculations[b]

	Cpd2			Cpd3			Cpd4		
	$\Delta E^{d\to q}$	$\Delta G^{d\to q}$	$\langle S^2\rangle$	$\Delta E^{d\to q}$	$\Delta G^{d\to q}$	$\langle S^2\rangle$	$\Delta E^{d\to q}$	$\Delta G^{d\to q}$	$\langle S^2\rangle$
BP86	−13.1	−12.6	0.76/3.75	−13.3	−14.0	0.76/3.75	−10.6	−11.7	0.77/3.75
TPSS	−15.9	−15.6	0.76/3.75	−16.2	−15.4	0.76/3.75	−13.4	−14.3	0.78/3.75
PBE	−12.3	−12.5	0.76/3.75	−13.6	−13.8	0.76/3.75	−10.8	−11.0	0.77/3.75
B3LYP	−16.4	−16.6	0.76/3.75	−16.4	−17.2	0.76/3.75	−16.2	−16.7	0.76/3.75
B3PW91	−16.4	−16.5	0.76/3.75	−16.6	−16.3	0.76/3.75	−16.0	−16.8	0.76/3.75
BHandHLYP	−19.6	−19.6	0.76/3.75	−14.8	−14.9	0.76/3.75	−18.7	−19.4	0.76/3.75
	ΔE^{gr}_{cpd2}			ΔE^{gr}_{cpd3}			ΔE^{gr}_{cpd4}		
	SPP	LPP	$\Delta\Delta E^{gr}$	SPP	LPP	$\Delta\Delta E^{gr}$	SPP	LPP	$\Delta\Delta E^{gr}$
B3PW91	0.0	0.0	0.0	−54.0	−53.8	0.2	−44.6	−44.7	−0.1

[a] $\Delta E^{d\to q} = E^q - E^d$, $\Delta G^{d\to q} = G^q - G^d$. [b] Ground state (quartet in SPP and singlet in LPP calculations) energy differences $\Delta E^{gr}_{cpd3} = E^{gr}_{cpd3} - (E^{gr}_{cpd2} + E_{CO_2})$ and $\Delta E^{gr}_{cpd4} = E^{gr}_{cpd4} - (E^{gr}_{cpd2} + E_{CS_2})$. $\Delta\Delta E^{gr}$ is the difference of ΔE^{gr} between the SPP and LPP values, i.e., $\Delta\Delta E^{gr} = \Delta\Delta E^{gr}_{LPP} - \Delta\Delta E^{gr}_{SPP}$.

Table 2. Population Analysis of Cpd2, Cpd3, and Cpd4 with U Treated with SPP and LPP

		Cpd2		Cpd3		Cpd4	
		SPP	LPP	SPP	LPP	SPP	LPP
atomic charge[a]	U	1.4(1.4)	1.5	1.4(1.3)	1.5	1.2(1.0)	1.4
	C^{8c}	−0.7(−1.0)	−0.8	−0.5(−0.6)	−0.5	−0.4(−0.5)	−0.4
	E^{10c}			−0.6(−0.7)	−0.6	−0.1(0.01)	−0.2
	E^{11c}			−0.5(−0.7)	−0.6	−0.1(0.01)	−0.2
	C^{9c}			0.7(0.9)	0.6	−0.2(−0.3)	−0.2
bond order[b]	$U-N^{2d}$	0.28(0.31)	0.27	0.28(0.32)	0.27	0.30(0.32)	0.29
	$U-C^8$	0.63(0.47)	0.61				
	$U-E^{10}$			0.38(0.36)	0.37	0.52(0.60)	0.38
	$U-E^{11}$			0.40(0.36)	0.40	0.53(0.60)	0.39
	C^9-E^{10}			1.36(1.36)	1.37	1.36(1.43)	1.38
	C^9-E^{11}			1.40(1.38)	1.40	1.37(1.43)	1.38
	C^9-C^8			0.95(0.96)	0.94	0.96(0.99)	0.97

[a] Atomic charge from Mulliken and NBO (in parentheses) population analysis. [b] Mayer bond order and Wiberg bond index (in parentheses). [c] C^8 is the C atom that is bonded to U in Cpd2. E = O, S. C^9 is the C atom in CO_2 and CS_2. [d] In our calculations, the six U−N bonds have essentially the same bond orders; thus, only the values of the first $U-N^2$ bond are given here.

which are −53.8 (LPP) vs −54.0 (SPP) kcal/mol for eq 1 and −44.7 (LPP) vs −44.6 (SPP) kcal/mol for eq 2. This lends more confidence to the application of LPP treatment of the central U atom in the current model systems.

B. Functionalization of CO_2 and CS_2. According to the experimental study,[6] the functionalization of CO_2 and CS_2 starts with the formation of a stable uranium(III) alkyl complex, Cpd2, which may undergo an insertion reaction of CO_2 or CS_2 to give a dicarboxylate (Cpd3) or a dithiocarboxylate (Cpd4) species, respectively.

Different from an earlier study[38] where the uranium is six-coordinated with a bulky ligand [$(^{Ad}ArO)_3tacn$, with $(^{Ad}ArOH)_3tacn$ =1,4,7-tris(3-adamantyl-5-*tert*-butyl- 2-hydroxybenzyl)1,4,7-triazacyclononane] and has the ability to accommodate a CO_2 molecule in an η^1 fashion, in Cpd2, however, the U atom has a coordination number of 7, where the seventh coordination site is occupied by a benzyl group and the surrounding region is crowded by two macrocyclic ligands (Tp*). Thus, there is no space accessible for CO_2 or CS_2 to attach to the central metal in the η^1 mode. For this reason, in our calculations, we did not locate a complex with a CE_2 (E = O, S) molecule coordinated to uranium, and the activation of CE_2 will have to compete with the retainment of the $U-C^8$ bond (see Figure 1 for the numbering of key atoms).

Formation of Cpd3. As seen in Figure 3, the functionalization of CO_2 promoted by Cpd2 proceeds in a stepwise manner. During the first step, the CO_2 interacts with the methylene group of the benzyl ligand to form the C^8-C^9 bond. In the meantime, the $U-C^8$ bond is broken (distance goes from 2.555 Å in RC to 2.720 Å in TS1 to 4.413 Å in IM), and in the intermediate (IM) the seventh coordination site is occupied by one of the oxygen atoms (here O^{10}) of CO_2 with a $U-O^{10}$ distance of 2.252 Å. The located transition state TS1 features the presence of a single imaginary frequency of 195i cm^{-1}, corresponding to the stretching of $U-C^8$, $U-O^{10}$, and C^9-C^8 bonds and the bending of O═C═O, i.e., $0.77R^{C^9-C^8} + 0.33R^{U^1-O^{10}} - 0.24R^{U^1-C^8} + 0.36A^{O^{11}-C^9-O^{10}}$ (only vectors with major contributions are shown here), which suggests that the insertion of CO_2 into the $U-C^8$ bond is a concerted process. In TS1, O^{10} weakly interacts with the U atom (2.666 Å), and this perturbs the C^9-O^{10} bond, which elongates from 1.168 Å in RC to 1.190 Å in TS1.

The second step realizes the coordination of the newly formed $PhCH_2CO_2^-$ ligand to uranium in a κ^2 mode by a reorientation of its $-COO^-$ side chain. In the product Cpd3, the two oxygen atoms have essentially the same distances to atoms U (2.490 vs 2.491 Å) and C^9 (1.272 vs 1.267 Å), indicating a similar bond strength of $U-O^{10}$ and $U-O^{11}$.

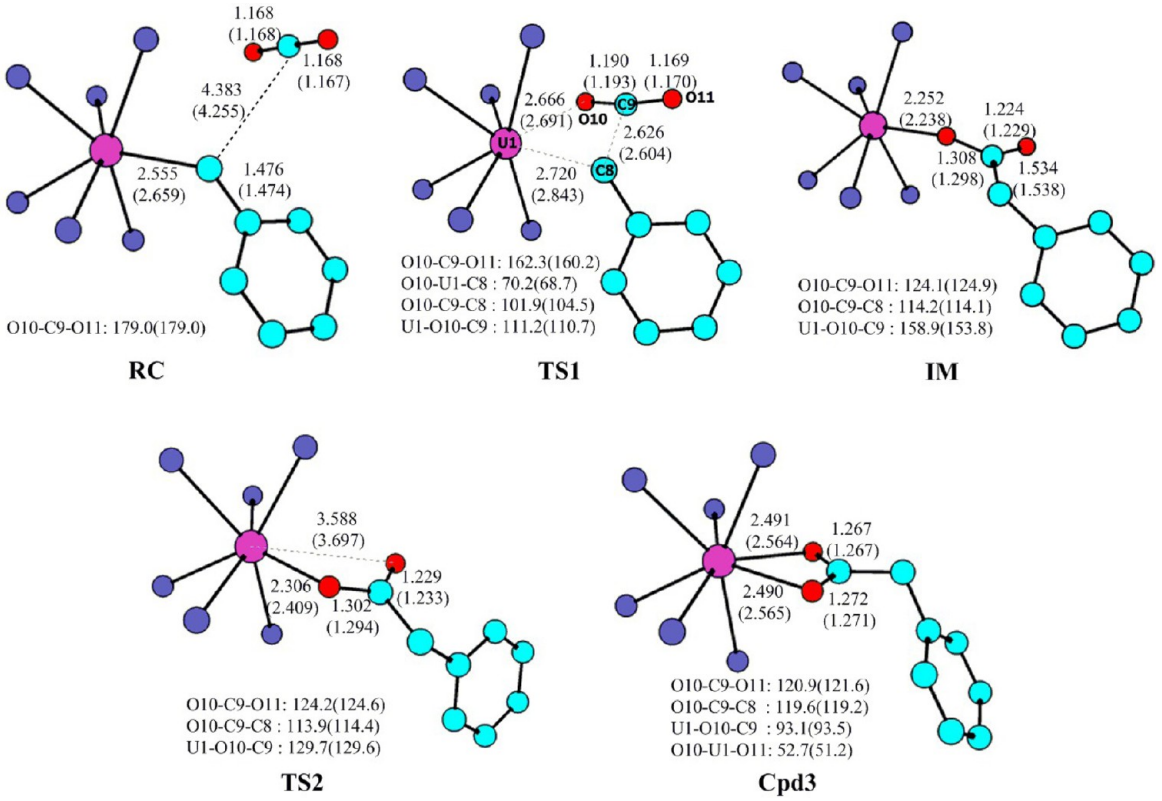

Figure 3. Stationary points on the pathway of the catalyzed functionalization of CO_2 with key geometric parameters from SPP and LPP (in parentheses) calculations. Only atoms relevant directly to the discussions are shown for simplicity, and the color scheme for the representation of the atoms is N (*blue*), U (*magenta*), O (*red*), and C (*cyan*).

The potential energy profile is shown in Figure 4. The first step, i.e., the insertion of CO_2, is the rate-determining step with an energy barrier of about 10 kcal/mol. This step is strongly exothermic by about 50 kcal/mol. Concerning the bonds formed during this step, the σ_{C-C}, the U−O dative bond compared to those cleaved, the π_{C-O}, and the U−C bonds, it is conceivable that the insertion of CO_2 into the U−C bond is a thermally favorable process. The subsequent reorientation of the $PhCH_2COO^-$ side chain requires an energy of 2.5 kcal/mol, and the formation of the second U−O^{11} bond gains an energy of 6.0 kcal/mol to stabilize the product.

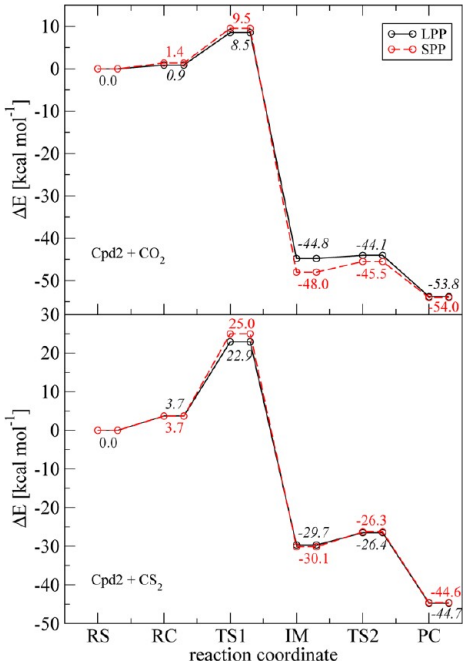

Figure 4. Energy profiles for the catalyzed functionalization of CO_2 and CS_2. PC represents Cpd3 in the reaction of Cpd2 + CO_2 and Cpd4 in that of Cpd2 + CS_2.

The moderate exothermicity of the formation of the U−O^{11} bond indicates that it does not contribute much to the stabilization of the product because, besides the possible presence of steric repulsive interaction between the phenylacetic group and the Tp* ligands, it needs to compensate the energy loss from the weakening of the existing U−O^{10} bond. As seen in Figure 3, in IM, the bond length of U−O^{10} is 2.252 Å, while it increases to 2.490 Å in Cpd3 where the O^{11} atom is attached to U atom.

Through the reaction, in SPP calculations, the spin density on the U atom is calculated to be 3.1 and keeps constant; thus, in Figure 5 we only plotted the Mulliken atomic charge and Mayer bond order (MBO) of key atoms and bonds to show how these quantities fluctuate along the reaction. It is clear that during the reaction, there is charge transfer from the methylene of the benzyl group and, less significantly, the U atom to the O atoms. Regarding the bonding modes of the O atoms, consistent with the observations in geometry (Figure 3), the MBO of U−O^{10} increases during the first step, while it moderately descreases when the U−O^{11} bond forms.

Formation of Cpd4. The functionalization of CS_2 proceeds in a similar way to that of CO_2 (Figure 6), i.e., the insertion of CS_2 into the U−C^8 bond happens first, and the imaginary frequency of TS1, 186i cm^{-1}, corresponds to a vibrational mode of $0.78R^{C^8-C^9} - 0.40R^{U^1-C^8} + 0.23R^{U^1-S^{10}}$ with only vectors with

dx.doi.org/10.1021/ct300075n | *J. Chem. Theory Comput.* 2012, 8, 3605−3617

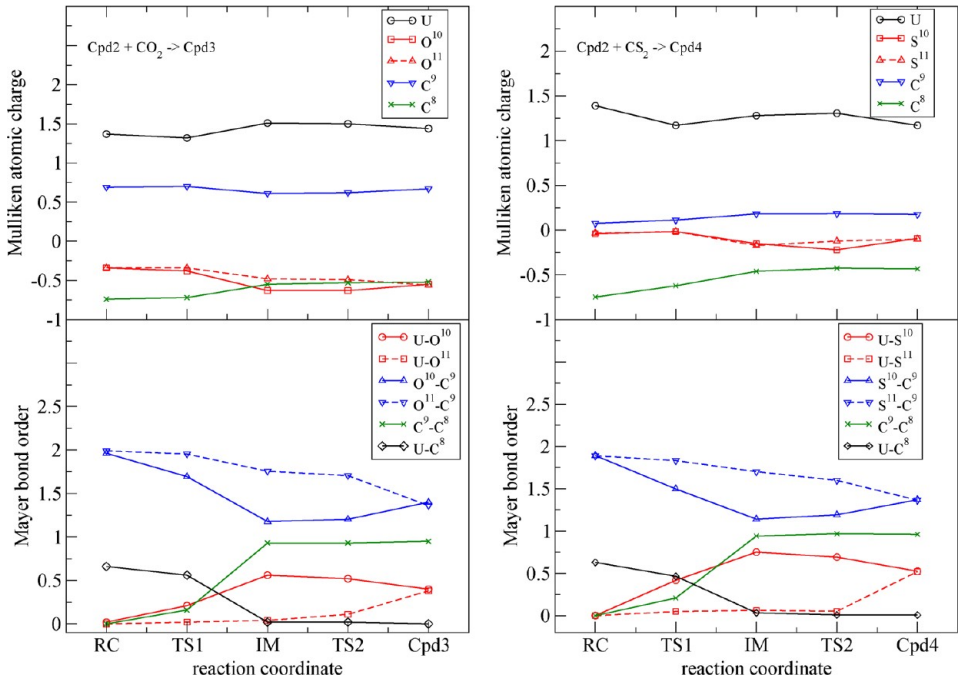

Figure 5. Fluctuations in the Mülliken atomic charge and Mayer bond order toward the formation of Cpd3 (left panel) and Cpd4 (right panel).

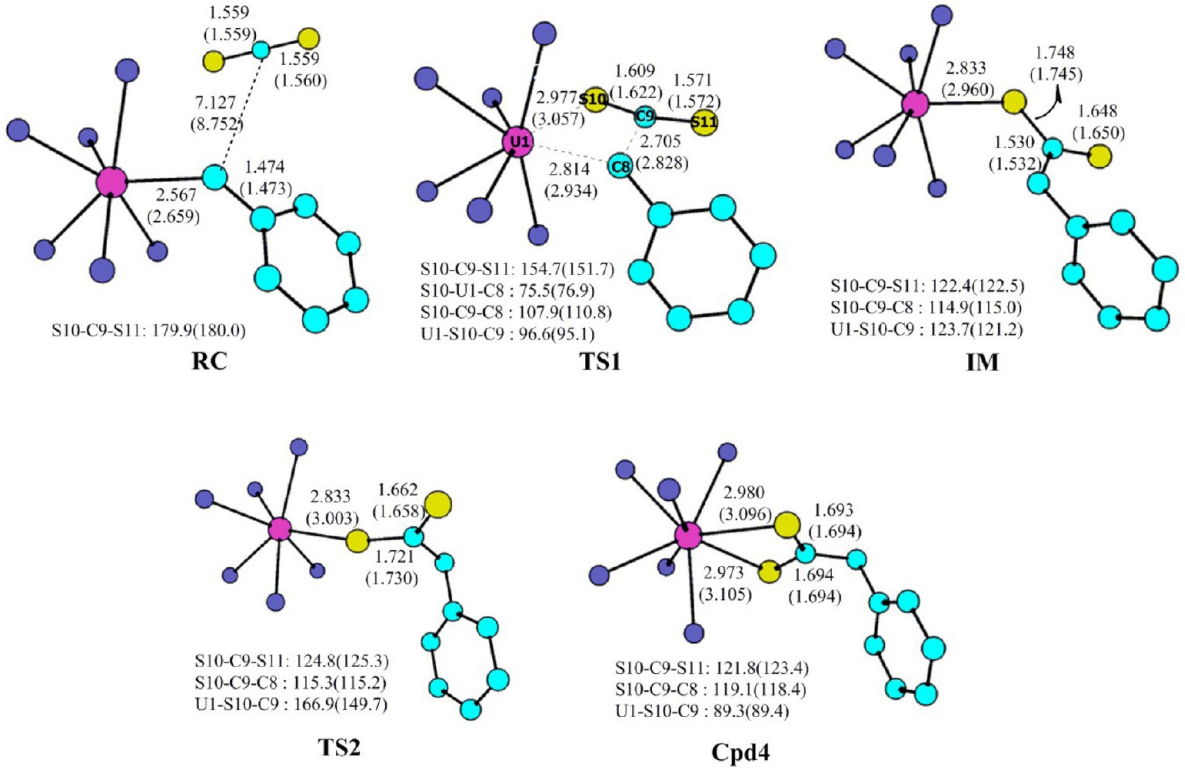

Figure 6. Stationary points on the pathway of the catalyzed functionalization of CS_2 with key geometric parameters from SPP and LPP (in parentheses) calculations. The representation of atoms is the same as in Figure 3 except for S, which is shown in *goldenrod*.

major contributions being shown. This is followed by a reorientation of the $PhCH_2CS_2^-$ ligand to produce a $(Tp^*)_2U$-κ^2-S_2CCH_2Ph complex (Cpd4).

However, in view of energies, the insertion of CS_2 into the $U-C^8$ bond is much more demanding than that of CO_2, and the energy required to overcome the barrier is up to 25.0 kcal/mol (Figure 4) with an exothermicity of 30.1 kcal/mol. The folding of the $-CS_2^-$ side chain is a facile process, and the formation of a second U−S bond brings a stabilization energy of 14.5 kcal/mol.

The lesser exothermicity in the functionalization of CS_2 than that of CO_2 suggests a weaker U−S interaction compared to the U−O bond. According to our calculation, the U−O has more ionic features (q_U = 1.4*e*, q_O = −0.5 to −0.6*e*) than the U−S bond (q_U = 1.2*e*, q_S = −0.1*e*). In view of Mayer bond order

dx.doi.org/10.1021/ct300075n | *J. Chem. Theory Comput.* 2012, 8, 3605−3617

(MBO, Table 2), the U−O bond in Cpd3 has an MBO of 0.38−0.40, while the U−S in Cpd4 has a value of 0.52−0.53. The larger MBO of the U−S bond is mainly due to the back-donation of the lone-pair electrons of the S atom to the U atom.

In Table 3, we collected the relative free energies and relative enthalpies for the reactions of Cpd3/Cpd4 formation to analyze the contribution of entropy. As we expected, the contribution of entropy raises the barrier of the first step, which involves the loss of degree of freedom of the CO_2 or the CS_2 molecules, to about 20 kcal/mol in the CO_2 case or more than 30 kcal/mol in the CS_2 case. However, this does not change the mechanisms described by the electronic energy profile.

Table 3. Relative Free Energies and Relative Enthalpies (kcal/mol) for the Formation of Cpd3 and Cpd4 in Their Quartet States from SPP and LPP Calculations

	CO_2		CS_2	
	ΔG (SPP/LPP)	ΔH (SPP/LPP)	ΔG (SPP/LPP)	ΔH (SPP/LPP)
RS[a]	0.0/0.0	0.0/0.0	0.0/0.0	0.0/0.0
RC	7.0/7.4	2.2/1.6	8.5/9.6	4.4/4.4
TS1	20.6/19.8	9.0/8.1	36.8/35.3	24.7/22.4
IM	−38.2/−35.1	−48.8/−45.5	−20.3/−20.3	−30.4/−29.8
TS2	−36.9/−33.6	−46.3/−45.2	−15.8/−14.8	−27.0/−27.2
PC[b]	−45.4/−44.3	−54.6/−54.5	−33.3/−32.5	−45.0/−45.3

[a]RS: reactant state with energy calculated from the summation of two components contributed from Cpd2 and CO_2 or CS_2. [b]PC is Cpd3 in the CO_2 case and Cpd4 in the CS_2 case.

For comparison, the TPSS functional was also employed to obtain the energy profiles for the formation of Cpd3 and Cpd4, and the results are consistent with those from B3PW91 calculations. Using the TPSS method, the functionalization of CO_2 is also found to be a two-step process, and TS1 has an energy of 5.8/4.5 (SPP/LPP) kcal/mol, which is moderately smaller than that from B3PW91 calculations of 9.5/8.5 kcal/mol. The reaction then proceeds to an intermediate (IM) with an energy of −44.2/−43.2 (SPP/LPP) kcal/mol, which is followed by TS2 with −41.2/−42.2 kcal/mol, and ends up with Cpd3 with an energy of −52.6/−52.4 kcal/mol. In the functionalization of CS_2, these values change to 19.0/16.5, −28.9/−28.3, −23.6/−24.6, and −43.9/−42.7 kcal/mol for TS1, IM, TS2, and Cpd4, respectively. The corresponding data from B3PW91 calculations are 25.0/22.9, −30.1/−29.7, −26.3/−26.4, and −44.6/−44.7 kcal/mol. It is clear that TPSS and B3PW91 methods predict the same reaction mechanism for the functionalization of CO_2/CS_2, with the first step as the rate-determining step.

C. Consumption of Cpd3 and Cpd4. According to experimental studies,[6] in the presence of TMSI, Cpd3 is consumed to give products $Me_3SiOC(O)CH_2Ph$ and $(Tp^*)_2UI$ (denoted as Cpd1), while Cpd4 decomposes without reacting with the TMSI. The difference in the propensity of Cpd3 and Cpd4 in the reaction with TMSI is due to the nature of the U−E (E = O, S) bond. As mentioned above (Table 2 and Figure 5), the U−O bond is more ionic than the U−S bond, and the O atom has a stronger nucleophilicity than the S atom, which may facilitate the electrophilic attack of TMSI.

In our calculations, the reaction of Cpd3 with TMSI is found to proceed along a three-step pathway (Figure 7), and one U−O bond (U−O^{11}) dissociates prior to the formation of the O−Si

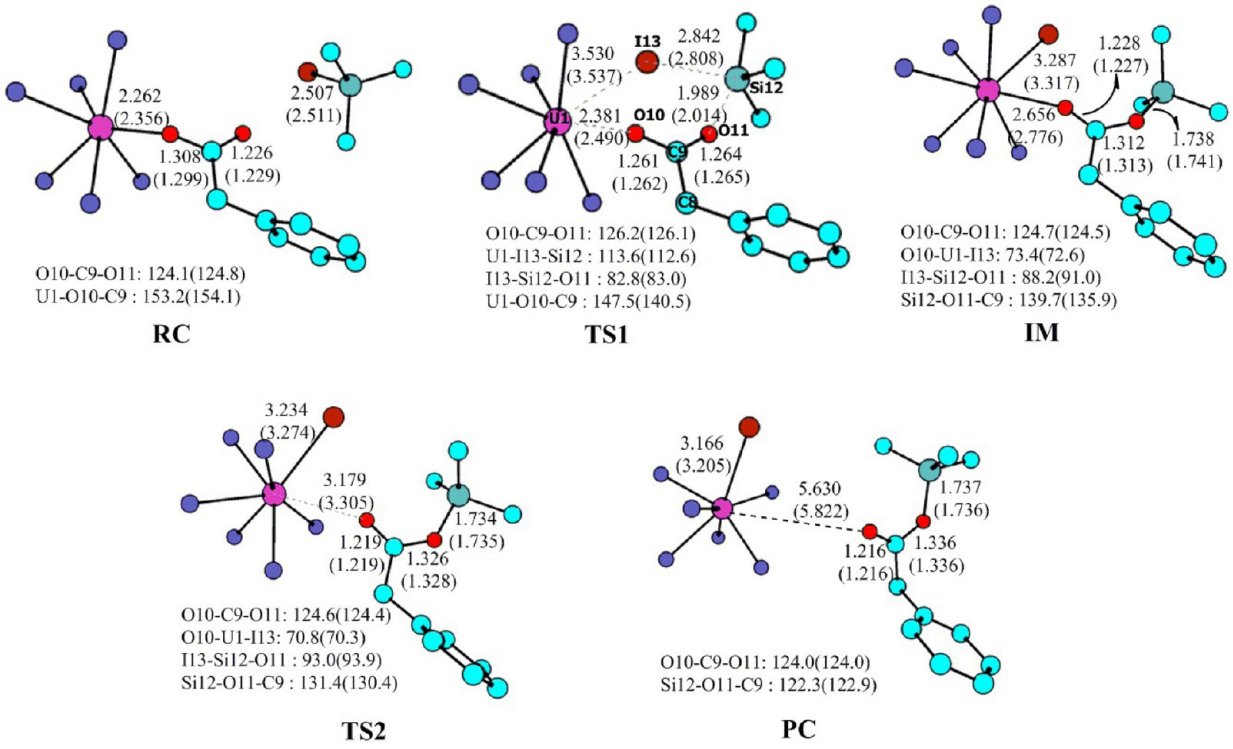

Figure 7. Stationary points on the pathway of Cpd3 consumption by Me_3SiI with key geometric parameters from SPP and LPP (in parentheses) calculations. Only the geometric parameters from calculations in which the I atom was described by SDD(aVTZ) basis set are shown. The first step of the reaction is the reverse reaction of the second step in the formation of Cpd3 (Figure 3), thus not shown for simplicity, and accordingly the $(Tp^*)_2U(\eta^1-OC(O)CH_2Ph)$ complex is denoted as RC here. The representation of atoms is the same as in Figure 3 except for Si, which is shown in *green*, and I, in *dark red*.

dx.doi.org/10.1021/ct300075n | J. Chem. Theory Comput. 2012, 8, 3605−3617

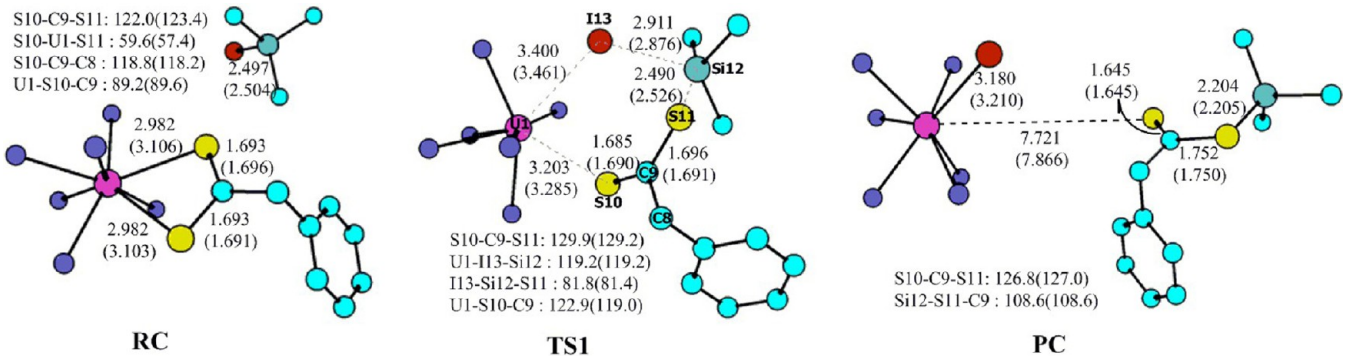

Figure 8. Stationary points on the pathway of the Cpd4 consumption by Me_3SiI with key geometric parameters from SPP and LPP (in parentheses) calculations. Only the geometric parameters from calculations in which the I atom was described by SDD(aVTZ) basis set are shown. The representation of atoms is the same as in Figure 6 except for Si, which is shown in *green*, and I, in *dark red*.

bond to give the intermediate with the U atom interacting with $PhCH_2CO_2^-$ in an η^1 mode (RC in Figure 7 with a U−O^{10} distance of 2.262 Å). The TMSI then approaches the released O^{11} atom to form an O^{11}−Si bond, and the I−Si bond is concomitantly weakened as the iodine atom moves to the U atom. This step is calculated to have an energy barrier of 17.3 (SPP) and 20.6 (LPP) kcal/mol and is exothermic by 5.1 (SPP) and 4.0 (LPP) kcal/mol. The final step is the dissociation of the U−O bond to give the product $(Tp^*)_2UI + PhCH_2CO_2SiMe_3$, and it is a facile process with a barrier less than 1 kcal/mol in our calculations (SPP, 0.1 kcal/mol; LPP, 0.4 kcal/mol). Thermodynamically, it is moderately favorable by an exothermicity of 3.5 (SPP) and 2.1 (LPP) kcal/mol.

In contrast, the reaction between Cpd4 and TMSI is found to be a concerted process (Figure 8) with an energy barrier of 40.6 (SPP) and 38.4 (LPP) kcal/mol. This value is significantly higher than that of the reaction of Cpd3 with TMSI. Since the U−S bond is weaker than the U−O bond, the higher barrier inherent in the reaction of Cpd4 with TMSI is not due to the cleavage of the U−S bond but the formation of the S−Si bond. Compared to the O atom, both S and Si atoms have relatively loosely bound outer shell electrons, but with relatively close electronegativities, χ, of 2.58 and 1.90, respectively (Pauling electronegativity[76−78]). These values are much smaller than that of the O atom, which is 3.44. The magnitude of the electronegativity difference, $\Delta\chi$, for O−Si and S−Si pairs determines their distinct behaviors in bond formation.

D. Uncatalyzed Reactions. To evaluate the role of trivalent uranium in the silyl(dithio)esterification of phenyl (dithio)acetic acid (PA and PTA), we have also investigated the reactions of TMSI with PA and PTA anions (PA^- and PTA^-) and their protonated neutral counterparts (HPA and HPTA), i.e., we consider a possible equilibrium below between the protonated and deprotonated states of PA and PTA, depending on the pH of the solution

$$\text{PA: HPA} \rightleftharpoons \text{PA}^- + \text{H}^+ \quad (3)$$

$$\text{PTA: HPTA} \rightleftharpoons \text{PTA}^- + \text{H}^+ \quad (4)$$

Reaction of PA with TMSI. The reaction of PA with TMSI may happen in the protonated (HPA) or deprotonated (PA^-) form of PA, depending on the pH value of the solution. We have thus studied the reaction of TMSI with PA in its two charge states. The energy profiles are plotted in Figure 9, and the fully optimized structures of the stationary points with selected key geometric parameters are shown in Figure 10.

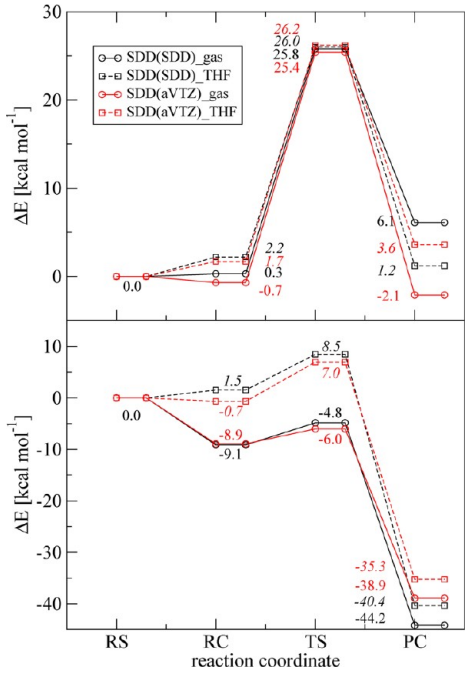

Figure 9. Energy profiles for the reactions of PA with Me_3SiI in its neutral (HPA, upper panel) and anionic states (PA^-, lower panel).

According to our calculation, in its neutral state, the reaction of PA with TMSI is a concerted process. As seen in Figure 10, in RCa, the TMSI interacts with HPA through a hydrogen bond between the I atom and the hydroxyl group of HPA. The structure of the transition state, TSa here, elucidates how the proton is delivered to the I atom when the Si−I bond is cleaved and the Si−O bond is formed. In TSa, the atoms directly involved in the reaction, including Si, I, O^{10}, O^{11}, H^{14}, and C^9, construct a pentagon-shape active region, and the I···H^{14}···O^{10} occupies a lateral of the pentagon. The change of I−H^{14} distance captured at the three stages of the reaction is from 2.785 Å in RCa to 2.296 Å in TSa to 2.048 Å in PCa, as observed in the calculation where the I atom was described by SDD(SDD), which clearly demonstrates the building of strong interaction between I and H^{14} atoms with the progress of the reaction. Overall, the concerted process involves the cleavage of Si−I and O^{10}−H^{14} σ bonds and the C−O^{11} π bond and the formation of Si−O^{11} and I−H^{14} σ bonds and the C−O^{10} π bond. This makes the whole reaction a thermoneutral or moderately endothermic process.

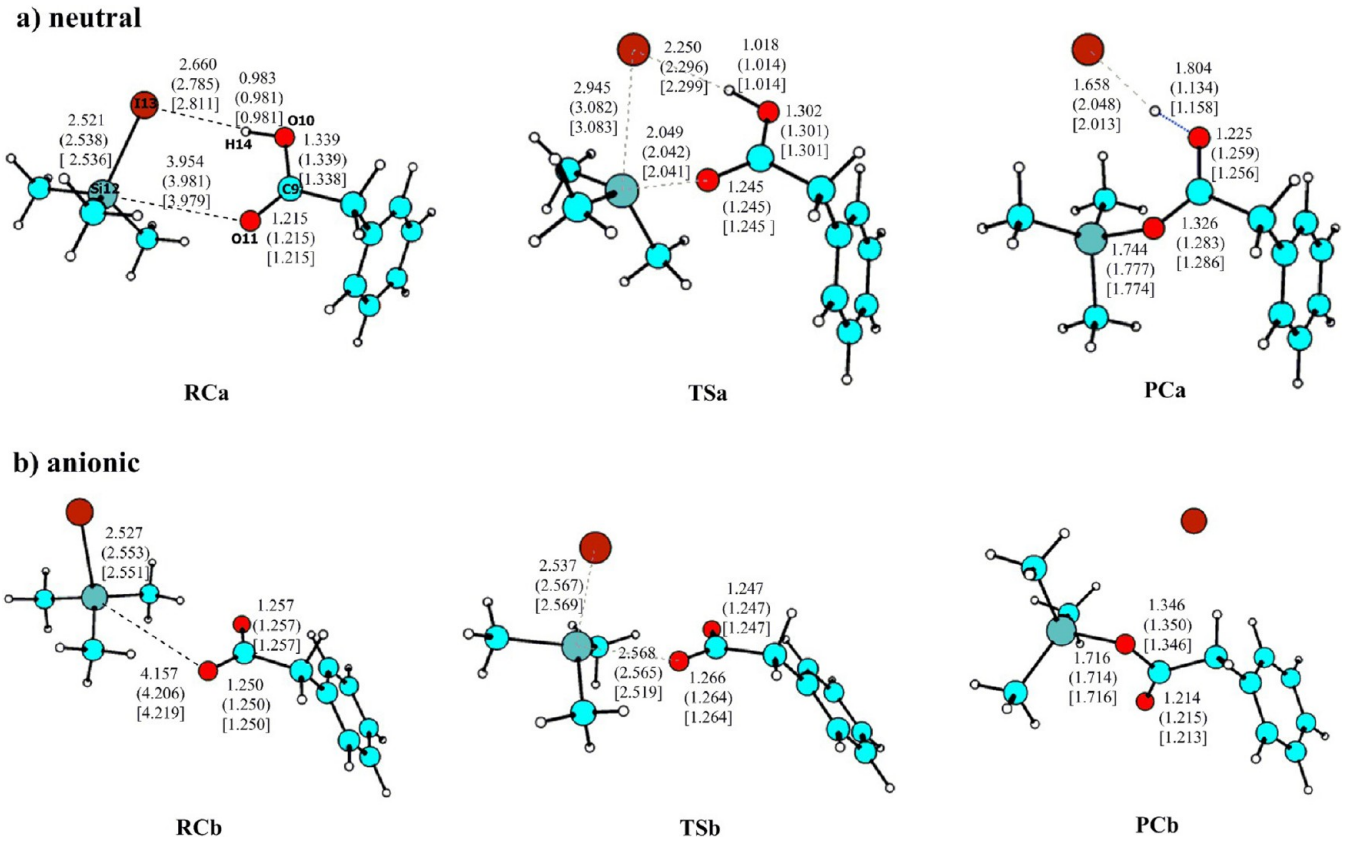

Figure 10. Stationary points in the reaction of PA with Me_3SiI at its (a) neutral (HPA) and (b) anionic (PA^-) states. Key geometric parameters shown are from B3PW91/6-31G(d) (I atom by SDD(aVTZ), (SDD(SDD)), and [LanL2DZ(LanL2DZ)]) calculations. The representation of atoms is the same as in Figure 7.

In view of energies (Figure 9), with a description of SDD(SDD) for the I atom, an energy of 25.8 kcal/mol is required to overcome the barrier, and this step is endothermic by 6.1 kcal/mol. Taking into account the solvent (THF) , the barrier changes to 26.0 kcal/mol. We have also refined the energies by using a larger basis set for the description of I with the valence shell described by aVTZ basis set and 6-31(d) for the other atoms, though this does not change the energies of the reaction much, and the calculated barrier is 25.4 kcal/mol in the gas phase and 26.2 kcal/mol in THF, with a reaction energy change of −2.1 and 3.6 kcal/mol, respectively.

The reaction in the anionic state of PA, i.e., PA^-, is found to be a much easier process. Similar to the reaction of HPA, the cleavage of the Si−I bond and the formation of the Si−O bond happen concertedly, and the calculated energy barrier is 4.3 kcal/mol relative to RC. With the inclusion of the solvent effect, the barrier increases to 7.0 kcal/mol, suggesting that in its anionic state, the solvent THF moderately disfavors the reaction between PA^- and TMSI. Energy refinement using an aVTZ basis set for the valence shell of the I atom gives a barrier of 2.9 kcal/mol in the gas phase and 7.7 kcal/mol when the solvent effect of THF is taken into account by means of the PCM model and thus does not change the results much.

The large difference in energies between the reactions in the neutral and anionic states of PA demonstrates the importance of a rich distribution of negative charge on the carboxylate group of PA and confirms the electrophilic feature of the attack of TMSI on PA.

It is interesting to note that the energy barrier inherent in the reaction of Cpd3 with TMSI lies between that of HPA and PA^-, i.e., $\Delta E^{\ddagger}$ (PA^-) < $\Delta E^{\ddagger}$ (Cpd3) < $\Delta E^{\ddagger}$ (HPA). This suggests that PA^- is more active toward the reaction with TMSI when coordinated to the trivalent U atom than being protonated. The higher barrier in the case of Cpd3, compared to PA^-, may be caused for two reasons: *First*, the steric hindrance due to the bulky ligands in Cpd3 blocks an easy approach of TMSI to the active site, and it is also difficult for the uranium atom to interact with iodine atom to activate the Si−I bond. *Second*, the U−η^1PA interaction stabilizes PA and makes the reaction toward TMSI less favorable. The composite effect of the two factors leads to a lower reactivity of Cpd3 toward TMSI compared to PA^-.

Reaction of PTA with TMSI. The reaction of PTA with TMSI follows a similar pathway to PA (Figure 11) but has a much higher activation energy, which is calculated to be, relative to RC, about 30 kcal/mol in its neutral state (HPTA) and around 20 kcal/mol in its anionic state (PTA^-, see Figure 12). The higher energy barriers suggest a lower reactivity of PTA toward TMSI which is consistent with the above explanation that the difference in the electronegativity between the two atoms that are to be bonded determines the feasibility of the bond formation process.

In the presence of a trivalent uranium complex $[(Tp^*)_2U]^+$, as discussed above, the reaction happens with an energy barrier of 40.6 (SPP) or 38.4 (LPP) kcal/mol, which is much higher than both cases of PTA in its neutral and anionic states. Thus, the coordination of PTA to trivalent uranium does not favor its silyldithioesterification toward TMSI. This is in contrast to the case of Cpd3. However, note that our calculations suggested a U−O dissociation step preceding to the O−Si bond formation in the case of Cpd3. The stepwise mechanism for the consumption of Cpd3 facilitates the reaction by diminishing the steric repulsion from the bulky ligands to the TMSI. This is not the case in Cpd4.

dx.doi.org/10.1021/ct300075n | *J. Chem. Theory Comput.* 2012, 8, 3605−3617

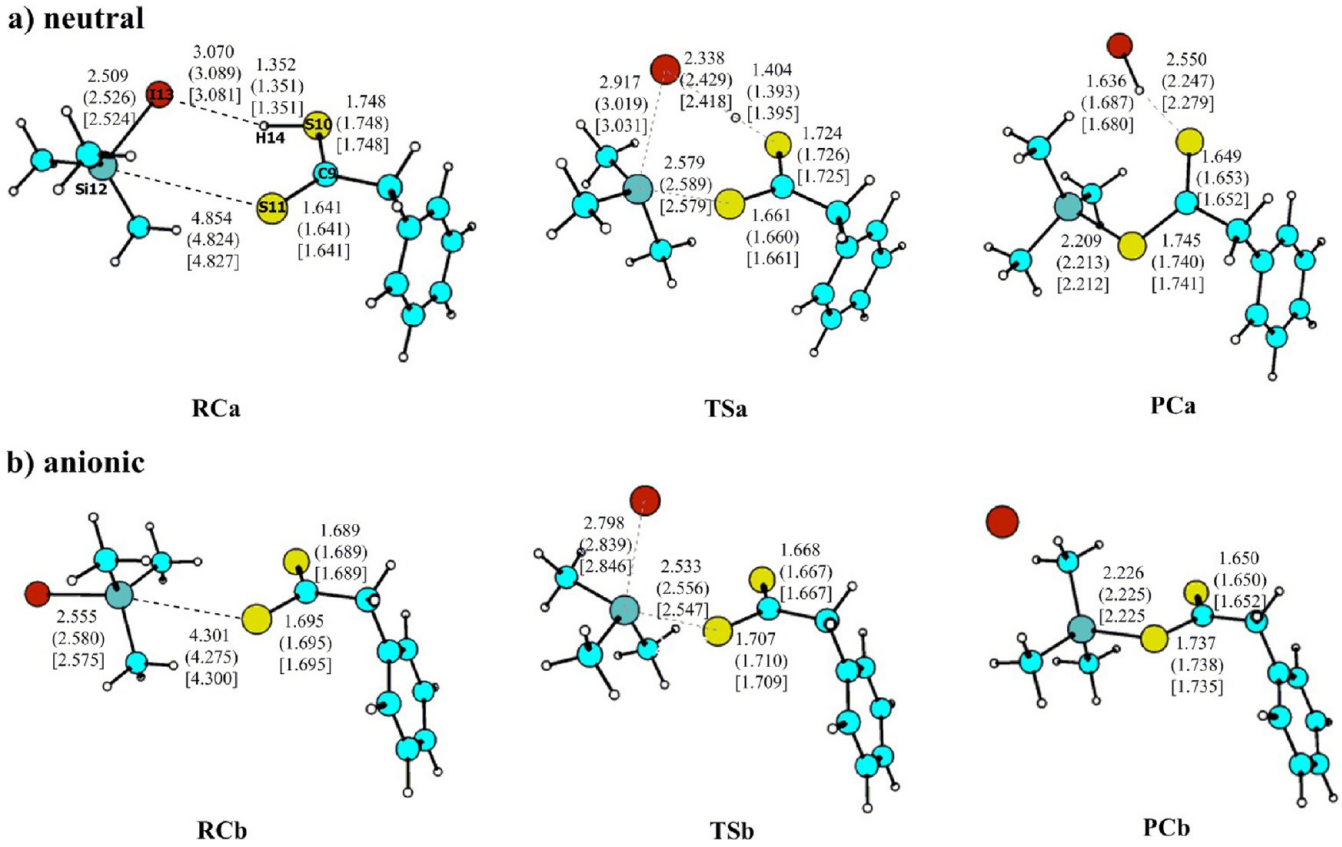

Figure 11. Structures of the stationary point in the reaction of PTA with Me_3SiI at its (a) neutral (HPTA) and (b) anionic (PTA^-) states. Key geometric parameters shown are from B3PW91/6-31G(d) (I atom by SDD(aVTZ), (SDD(SDD)), and [LanL2DZ(LanL2DZ)]) calculations. The representation of atoms is the same as in Figure 8.

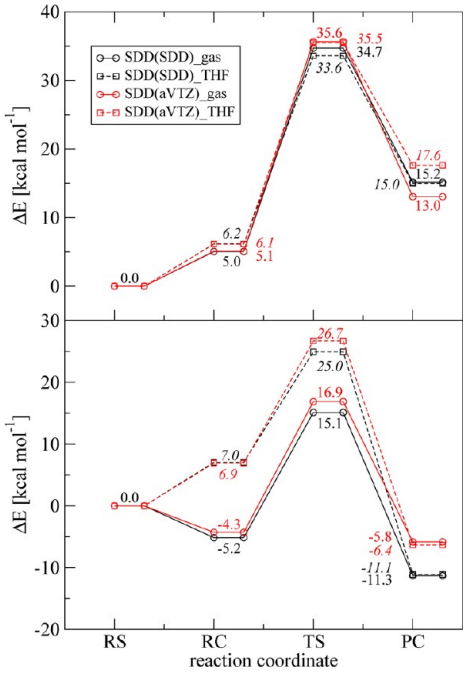

Figure 12. Energy profiles calculated for the reaction of PTA with Me_3SiI in its neutral (HPTA, upper panel) and anionic (PTA^-, lower panel) states.

Even though, in view of the energy profile of the Cpd4 formation (Figure 4), the dissociation of the $U-S^{11}$ bond, which is the reverse process of the second step, requires an energy of 18.3 kcal/mol and is not a facile process. In addition, due to the weaker electron-withdrawing ability of the S atom compared to the O atom, the released S atom can not benefit from the reducing U(III) moiety to have a rich negative charge distribution; thus the S−Si bond formation is still difficult.

On the basis of the analysis, we may draw a conclusion regarding the role of trivalent uranium in the silyl(dithio)esterification of PA/PTA that, depending on the electronegativity of the chalcogen atom of the (dithio)carboxylate group, the stronger the electronegativity, the easier it is for the reaction to happen.

It merits a discussion on the attack mode toward the formation of the O−Si or S−Si bond in the reaction of PA or PTA with TMSI. For a naked PA or PTA molecular system, i.e., without the presence of the trivalent U moiety, in principle, it is possible for the O atom of PA or the S atom of PTA to attack TMSI either from the front side, i.e., *cis* to the iodine atom, or from the back side, i.e., *trans* to the iodine atom. In the preceding part, we have only discussed the reactions following the front-side attack pathway in order to compare to the reactions with the presence of a uranium moiety.

When the reaction happens in the backside manner, it is a standard S_N2 reaction, i.e., the formation of the O/S−Si bond and the cleavage of the Si−I bond happen in a single step via a trigonal bipyramidal transition state. According to our calculations, the backside attack may proceed easily when PTA is deprotonated, while it is difficult when PA and PTA are protonated. For HPA and HPTA, due to the hygrogen bond interaction between the iodine atom and the proton of HPA and HPTA which anchors the TMSI, the frontside attack pathway is favored.

In deprotonated cases, we could not locate a transition state for the backside attack of PA^- to TMSI, partly due to the copresence

dx.doi.org/10.1021/ct300075n | *J. Chem. Theory Comput.* 2012, 8, 3605−3617

of a good leaving group (I atom, I−Si bond dissociation energy of 70.1 kcal/mol[78]) and a good attack group (O−Si bond energy of 191.2 kcal/mol[78]), but we did observe one for that of PTA^- to TMSI with an energy barrier of 10.1 kcal/mol at the level of B3PW91/6-31G(d)+SDD(aVTZ) with the solvent effect of THF included, and the whole reaction is exothermic by 6.4 kcal/mol, suggesting that the backside pathway is more favorable for PTA^- in the naked model system.

However, note that the chemical environment of the (dithio)-carboxylate group in Cpd3 and Cpd4 is more similar to that in HPA and HPTA, concerning the relatively ionic U−O/S bond compared to the H−O/S bond. Meanwhile, the frontside attack facilitates the formation of the U−I bond, which otherwise requires substantial energy for the I atom to migrate from one side of the trimethylsilyl plane (TMS) to another side in order to interact with the U atom.

CONCLUSION

With the B3PW91 functional, we have investigated the functionalization of CO_2 and CS_2 promoted by a trivalent uranium complex. The 5f-in-core treatment of uranium with 81 electrons in the core is found to be able to give good results comparable to those from the calculations with uranium treated by a quasi-relativistic small core ECP basis set.

According to our calculations, due to the high coordination number of the central uranium atom, which is 7 or 8, and the crowded assembly in the surrounding region, no complex with a direct interaction between U and CO_2 or CS_2 has been located prior to the insertion reaction, and the functionalization reaction proceeds via the competition between the formation of the U−E (E = O, S) bond and the retainment of U−C bond. This process is characterized as an exothermal process in both cases, and contains multiple steps. The first step involves the cleavage of the $U-C^8$ bond and the formation of the C^8-C^9 and $U-E^{10}$ bonds and requires an energy of 9.5 kcal/mol (SPP) for CO_2 and 25.0 kcal/mol (SPP) for CS_2 to overcome the barrier. Subsequently, the newly formed $PhCH_2CE_2^-$ group may reorient to form a second $U-O^{11}$ or $U-S^{11}$ dative bond which is characterized as a facile process with an energy barrier of 2.5 kcal/mol for CO_2 and 3.9 kcal/mol for CS_2.

Through the reaction, the SPP calculations show that the spin density mainly locates on the U atom and it keeps constant, while we do observe charge transfer from C^8 to O/S atoms. The U atom also contributes to the accumulation of negative charge on the chalcogen atoms during the functionalization; however, it displays only minor fluctuation in its atomic charge.

Regarding the consumption of Cpd3 and Cpd4 upon the addition of TMSI, due to the strong electronegativity of the O atom in Cpd3, Cpd3 benefits from the charge transfer from trivalent U and has a higher reactivity toward TMSI than Cpd4. It is worth noting that in our calculations, the reaction of Cpd3 with TMSI proceeds in a stepwise manner, while that of Cpd4 proceeds in a concerted pathway.

In summary, according to our calculations, the below conclusions may be drawn:

- The functionalization of CO_2 or CS_2 promoted by $(Tp^*)_2UCH_2Ph$ is a two-step process, and the insertion of CO_2 or CS_2 into the U−C bond happens during the first step, which is followed by a reorientation of the $PhCH_2CE_2^-$ (E = O, S) ligand to give the final products Cpd3 or Cpd4.
- Due to the steric hindrance of the bulky ligands, the incoming CO_2 and CS_2 molecules do not have direct contact with uranium prior to the insertion reaction.
- The LPP treatment of trivalent uranium is adequate to give reliable energy profiles consistent with those where uranium is treated with the SPP basis set. This is partially due to the inactive behavior of the 5f electrons during the reaction, leading to the 5f-in-core treatment a reasonable approximation for the model systems in the present study.

ASSOCIATED CONTENT

Supporting Information

Cartesian coordinates, energies, and frequencies of fully optimized stationary points. This information is available free of charge via the Internet at http://pubs.acs.org/.

AUTHOR INFORMATION

Corresponding Author

*E-mail: dwang@ihep.ac.cn, dingwanjian@bnu.edu.cn.

Notes

The authors declare no competing financial interest.

ACKNOWLEDGMENTS

This work was financially supported by the National Natural Science Foundation of China to W.D., grant number 21073013, and by the Chinese Academy of Sciences in the framework of a Frontier of Novelty program to D.W., grant numbers Y1515540U1 and Y2291810S3, which are gratefully acknowledged. Z.C. thanks National Natural Science Foundation of China for its support of Major Project of Nulcear Energy, grant number 91026000. Prof. S. C. Bart of Purdue University is acknowledged for providing us the crystallographic information file (cif) of Cpd4. Part of the calculations were done on the computational grids in the computer center of the Institute of High Energy Physics (IHEP) maintained by Drs. Jingyan Shi and Bowen Kan, in the Supercomputing Center of Chinese Academy of Sciences (SCCAS) and in the National Supercomputing Center in Tianjin (NSCC-TJ).

REFERENCES

(1) Fox, A. R.; Bart, S. C.; Meyer, K.; Cummins, C. C. Towards uranium catalysts. *Nature* **2008**, *455*, 341−349.

(2) Arnold, P. L. Uranium-mediated activation of small molecules. *Chem. Commun.* **2011**, *47*, 9005−9010.

(3) Bart, S. C.; Anthon, C.; Heinemann, F. W.; Bill, E.; Edelstein, N. M.; Meyer, K. Carbon Dioxide Activation with Sterically Pressured Mid- and High-Valent Uranium Complexes. *J. Am. Chem. Soc.* **2008**, *130*, 12536−12546.

(4) Lam, O. P.; Bart, S. C.; Kameo, H.; Heinemann, F. W.; Meyer, K. Insights into the mechanism of carbonate formation through reductive cleavage of carbon dioxide with low-valent uranium centers. *Chem. Commun.* **2010**, *46*, 3137−3139.

(5) Zuend, S. J.; Lam, O. P.; Heinemann, F. W.; Meyer, K. Carbon Dioxide Insertion into Uranium-Activated Dicarbonyl Complexes. *Angew. Chem., Int. Ed.* **2011**, *50*, 10626−10630.

(6) Matson, E. M.; Forrest, W. P.; Fanwick, P. E.; Bart, S. C. Functionalization of Carbon Dioxide and Carbon Disulfide Using a Stable Uranium(III) Alkyl Complex. *J. Am. Chem. Soc.* **2011**, *133*, 4948−4954.

(7) Brennan, J. G.; Andersen, R. A.; Zalkin, A. Chemistry of trivalent uranium metallocenes: electron-transfer reactions. Synthesis and characterization of $[(MeC_5H_4)_3U]_2E$ (E = S, Se, Te) and the crystal structures of hexakis(methylcyclopentadienyl)sulfidodiuranium and

tris(methylcyclopentadienyl)(triphenylphosphine oxide)uranium. *Inorg. Chem.* **1986**, *25*, 1761−1765.
(8) Sakakura, T.; Choi, J.-C.; Yasuda, H. Transformation of Carbon Dioxide. *Chem. Rev.* **2007**, *107*, 2365−2387.
(9) Darensbourg, D. J. Making Plastics from Carbon Dioxide: Salen Metal Complexes as Catalysts for the Production of Polycarbonates from Epoxides and CO_2. *Chem. Rev.* **2007**, *107*, 2388−2410.
(10) Sakakura, T.; Kohno, K. The synthesis of organic carbonates from carbon dioxide. *Chem. Commun.* **2009**, 1312−1330.
(11) Huang, K.; Sun, C.-L.; Shi, Z.-J. Transition-metal-catalyzed C-C bond formation through the fixation of carbon dioxide. *Chem. Soc. Rev.* **2011**, *40*, 2435−2452.
(12) Jessop, P. G.; Ikariya, T.; Noyori, R. Homogeneous Hydrogenation of Carbon Dioxide. *Chem. Rev.* **1995**, *95*, 259−272.
(13) Williams, C. M.; Johnson, J. B.; Rovis, T. Nickel-Catalyzed Reductive Carboxylation of Styrenes Using CO_2. *J. Am. Chem. Soc.* **2008**, *130*, 14936−14937.
(14) Tanaka, R.; Yamashita, M.; Nozaki, K. Catalytic Hydrogenation of Carbon Dioxide Using Ir(III)-Pincer Complexes. *J. Am. Chem. Soc.* **2009**, *131*, 14168−14169.
(15) Benson, E. E.; Kubiak, C. P.; Sathrum, A. J.; Smieja, J. M. Electrocatalytic and homogeneous approaches to conversion of CO_2 to liquid fuels. *Chem. Soc. Rev.* **2009**, *38*, 89−99.
(16) Federsel, C.; Boddien, A.; Jackstell, R.; Jennerjahn, R.; Dyson, P. J.; Scopelliti, R.; Laurenczy, G.; Beller, M. A Well-Defined Iron Catalyst for the Reduction of Bicarbonates and Carbon Dioxide to Formates, Alkyl Formates, and Formamides. *Angew. Chem., Int. Ed.* **2010**, *49*, 9777−9780.
(17) Mosconi, E.; De Angelis, F. DFT Investigation of Ligand-Based Reduction of CO_2 to CO on an Anionic Niobium Nitride Complex: Reaction Mechanism and Role of the Na^+ Counterion. *Organometallics* **2011**, *30*, 4838−4846.
(18) Huff, C. A.; Sanford, M. S. Cascade Catalysis for the Homogeneous Hydrogenation of CO_2 to Methanol. *J. Am. Chem. Soc.* **2011**, *133*, 18122−18125.
(19) Tanaka, R.; Yamashita, M.; Chung, L. W.; Morokuma, K.; Nozaki, K. Mechanistic Studies on the Reversible Hydrogenation of Carbon Dioxide Catalyzed by an Ir-PNP Complex. *Organometallics* **2011**, *30*, 6742−6750.
(20) Wang, W.; Wang, S.; Ma, X.; Gong, J. Recent advances in catalytic hydrogenation of carbon dioxide. *Chem. Soc. Rev.* **2011**, *40*, 3703−3727.
(21) Gomes, C. D. N.; Jacquet, O.; Villiers, C.; Thuéry, P.; Ephritikhine, M.; Cantat, T. A Diagonal Approach to Chemical Recycling of Carbon Dioxide: Organocatalytic Transformation for the Reductive Functionalization of CO_2. *Angew. Chem.* **2011**, *123*, 1−6.
(22) Zhou, M.; Zhou, Z.; Zhuang, J.; Li, Z. H.; Fan, K.; Zhao, Y.; Zheng, X. Carbon Dioxide Coordination and Activation by Niobium Oxide Molecules. *J. Phys. Chem. A* **2011**, *115*, 14361−14369.
(23) Zhang, C.; Wang, M.; Xue, L.; Fan, T.; Lin, Z. DFT Studies on Reactions of CO_2 with Niobium and Vanadium Nitride Complexes. *Organometallics* **2011**, *30*, 5911−5918.
(24) Correa, A.; Martin, R. Palladium-Catalyzed Direct Carboxylation of Aryl Bromides with Carbon Dioxide. *J. Am. Chem. Soc.* **2009**, *131*, 15974−15975.
(25) Ukai, K.; Aoki, M.; Takaya, J.; Iwasawa, N. Rhodium(I)-Catalyzed Carboxylation of Aryl- and Alkenylboronic Esters with CO_2. *J. Am. Chem. Soc.* **2006**, *128*, 8706−8707.
(26) Takaya, J.; Tadami, S.; Ukai, K.; Iwasawa, N. Copper(I)-Catalyzed Carboxylation of Aryl- and Alkenylboronic Esters. *Org. Lett.* **2008**, *10*, 2697−2700.
(27) Ohishi, T.; Nishiura, M.; Hou, Z. Carboxylation of Organoboronic Esters Catalyzed by N-Heterocyclic Carbene Copper(I) Complexes. *Angew. Chem., Int. Ed.* **2008**, *47*, 5792−5795.
(28) Yeung, C. S.; Dong, V. M. Beyond Aresta's Complex: Ni- and Pd-Catalyzed Organozinc Coupling with CO_2. *J. Am. Chem. Soc.* **2008**, *130*, 7826−7827.
(29) Ochiai, H.; Jang, M.; Hirano, K.; Yorimitsu, H.; Oshima, K. Nickel-Catalyzed Carboxylation of Organozinc Reagents with CO_2. *Org. Lett.* **2008**, *10*, 2681−2683.
(30) Evans, W. J.; Seibel, C. A.; Ziller, J. W. Organosamarium-Mediated Transformations of CO_2 and COS: Monoinsertion and Disproportionation Reactions and the Reductive Coupling of CO_2 to $[O_2CCO_2]^{2-}$. *Inorg. Chem.* **1998**, *37*, 770−776.
(31) Evans, W. J.; Miller, K. A.; Ziller, J. W. Synthesis of $(O_2CEPh)^{1-}$ ligands (E = S, Se) by CO_2 insertion into lanthanide chalcogen bonds and their utility in forming crystallographically characterizable organoaluminum complexes $[Me_2Al(\mu\text{-}O_2CEPh)]_2$. *Inorg. Chem.* **2006**, *45*, 424−429.
(32) Evans, W. J.; Rego, D. B.; Ziller, J. W.; DiPasquale, A. G.; Rheingold, A. L. Facile Insertion of CO_2 into Tetra- and Pentamethylcyclopentadienyl Lanthanide Moieties To Form $(C_5Me_4RCO_2)^-$ Carboxylate Ligands (R = H, Me). *Organometallics* **2007**, *26*, 4737−4745.
(33) Ochiai, B.; Endo, T. Carbon dioxide and carbon disulfide as resources for functional polymers. *Prog. Polym. Sci.* **2005**, *30*, 183−215.
(34) Aresta, M.; Nobile, C. F.; Albano, V. G.; Forni, E.; Manassero, M. New nickel-carbon dioxide complex: synthesis, properties, and crystallographic characterization of (carbon dioxide)-bis-(tricyclohexylphosphine)nickel. *J. Chem. Soc., Chem. Commun.* **1975**, 636−637.
(35) Aresta, M.; Nobile, C. F. (Carbon dioxide)bis(trialkylphosphine) nickel complexes. *J. Chem. Soc., Dalton Trans.* **1977**, 708−711.
(36) Herskovitz, T. Carbon dioxide coordination chemistry. 3. Adducts of carbon dioxide with iridium(I) complexes. *J. Am. Chem. Soc.* **1977**, *99*, 2391−2392.
(37) Lam, O. P.; Anthona, C.; Meyer, K. Influence of steric pressure on the activation of carbon dioxide and related small molecules by uranium coordination complexes. *Dalton Trans.* **2009**, 9677−9691.
(38) Castro-Rodriguez, I.; Nakai, H.; Zakharov, L. N.; Rheingold, A. L.; Meyer, K. A Linear, O-Coordinated η^1-CO_2 Bound to Uranium. *Science* **2004**, *305*, 1757−1759.
(39) Calderazzo, F.; Dell'Amico, G.; Netti, R.; Pasquali, M. Dialkylcarbamato complexes of transition elements. 1. A new method for the synthesis of N,N-dialkylcarbamato and N,N-dialkyldithiocarbamato complexes of uranium(IV). *Inorg. Chem.* **1978**, *17*, 471−473.
(40) Arduini, A. L.; Jamerson, J. D.; Takats, J. Reactivity of dicyclopentadienylbis(diethylamido)uranium(IV). Insertion reactions. *Inorg. Chem.* **1981**, *20*, 2474−2479.
(41) Moloy, K. G.; Marks, T. J. The insertion of carbon dioxide into actinide alkyl and hydride bonds. *Inorg. Chim. Acta* **1985**, *110*, 127−131.
(42) Lescop, C.; Arliguie, T.; Lance, M.; Nierlich, M.; Ephritikhine, M. Bispentamethylcyclopentadienyl uranium(IV) thiolate compounds. Synthesis and reactions with CO_2 and CS_2. *J. Organomet. Chem.* **1999**, *580*, 137−144.
(43) Evans, W. J.; Walensky, J. R.; Ziller, J. W. Insertion Reactivity of CO_2, PhNCO, $Me_3CC{\equiv}N$, and $Me_3CN{\equiv}C$ with the Uranium-Alkynyl Bonds in $(C_5Me_5)_2U(C{\equiv}CPh)_2$. *Organometallics* **2010**, *29*, 945−950.
(44) Evans, W. J.; Walensky, J. R.; Ziller, J. W. Reaction Chemistry of the U^{3+} Metallocene Amidinate $(C_5Me_5)_2[^iPrNC(Me)NiPr]U$ Including the Isolation of a Uranium Complex of a Monodentate Acetate. *Inorg. Chem.* **2010**, *49*, 1743−1749.
(45) Duhovic, S.; Khan, S.; Diaconescu, P. L. In situ generation of uranium alkyl complexes. *Chem. Commun.* **2010**, *46*, 3390−3392.
(46) Korobkov, I.; Gorelsky, S.; Gambarotta, S. Reduced Uranium Complexes: Synthetic and DFT Study of the Role of π Ligation in the Stabilization of Uranium Species in a Formal Low-Valent State. *J. Am. Chem. Soc.* **2009**, *131*, 10406−10420.
(47) Antunes, M. A.; Ferrence, G. M.; Domingos, A.; McDonald, R.; Burns, C. J.; Takats, J.; Marques, N. Uranium (III) Scorpionates:2009 Synthesis and Structure of $[(TpMe_2)_2U\{N(C_6H_5)_2\}]$ and $[(TpMe_2)_2U\text{-}\{N(SiMe_3)_2\}]$. *Inorg. Chem.* **2004**, *43*, 6640−6643.
(48) Antunes, M. A.; Domingos, A.; dos Santos, I. C.; Marques, N.; Takats, J. Synthesis and characterization of uranium(III) compounds supported by the hydrotris(3,5-dimethyl-pyrazolyl)borate ligand: Crystal structures of $[U(Tp^{Me2})_2(X)]$ complexes (X = OC_6H_2−2,4,6-Me_3, dmpz, Cl). *Polyhedron* **2005**, *24*, 3038−3045.

(49) Matson, E. M.; Fanwick, P. E.; Bart, S. C. Formation of Trivalent U-C, U-N, and U-S Bonds and Their Reactivity toward Carbon Dioxide and Acetone. *Organometallics* **2011**, *30*, 5753−5762.
(50) Becke, A. D. A new mixing of Hartree-Fock and local density-functional theories. *J. Chem. Phys.* **1993**, *98*, 1372−1377.
(51) Perdew, J. P. Unified Theory of Exchange and Correlation Beyond the Local Density Approximation. In *Electronic Structure of Solids '91*; Ziesche, P., Eschrig, H., Eds.; Akademie Verlag: Berlin, 1991; pp 11−20.
(52) Moritz, A.; Cao, X.; Dolg, M. Quasirelativistic energy-consistent 5f-in-core pseudopotentials for trivalent actinide elements. *Theor. Chem. Acc.* **2007**, *117*, 473−481.
(53) Küchle, W.; Dolg, M.; Stoll, H.; Preuss, H. Energy-adjusted pseudopotentials for the actinides. Parameter sets and test calculations for thorium and thorium monoxide. *J. Chem. Phys.* **1994**, *100*, 7535−7542.
(54) Cao, X.; Dolg, M.; Stoll, H. Valence basis sets for relativistic energy-consistent small-core actinide pseudopotentials. *J. Chem. Phys.* **2003**, *118*, 487−496.
(55) Cao, X.; Dolg, M. Segmented contraction scheme for small-core actinide pseudopotential basis sets. *THEOCHEM* **2004**, *673*, 203−209.
(56) Bergner, A.; Dolg, M.; Kuechle, W.; Stoll, H.; Preuss, H. Ab-initio energy-adjusted pseudopotentials for elements of groups 13−17. *Mol. Phys.* **1993**, *80*, 1431−1441.
(57) Martin, J. M. L.; Sundermann, A. Correlation consistent valence basis sets for use with the StuttgartDresdenBonn relativistic effective core potentials: The atoms GaKr and InXe. *J. Chem. Phys.* **2001**, *114*, 3408−3420.
(58) Hay, P. J.; Wadt, W. R. Ab initio effective core potentials for molecular calculations - potentials for the transition-metal atoms Sc to Hg. *J. Chem. Phys.* **1985**, *82*, 270−283.
(59) Wadt, W. R.; Hay, P. J. Ab initio effective core potentials for molecular calculations - potentials for main group elements Na to Bi. *J. Chem. Phys.* **1985**, *82*, 284−298.
(60) Hay, P. J.; Wadt, W. R. Ab initio effective core potentials for molecular calculations - potentials for K to Au including the outermost core orbitals. *J. Chem. Phys.* **1985**, *82*, 299−310.
(61) Banik, N. L.; Schimmelpfennig, B.; Marquardt, C. M.; Brendebach, B.; Geist, A.; Denecke, M. A. Characterization of redox sensitive plutonium(III) complexed with alkylated 2,6-ditriazinylpyridine (BTP) in organic solution. *Dalton Trans.* **2010**, *39*, 5117−5122.
(62) Castro, L.; Yahia, A.; Maron, L. Are 5f Electrons Really Active in Organoactinide Reactivity? Some Insights from DFT Studies. *ChemPhysChem* **2010**, *11*, 990−994.
(63) Manni, G. L.; Walensky, J. R.; Kraft, S. J.; Forrest, W. P.; Perez, L. M.; Hall, M. B.; Gagliardi, L.; Bart, S. C. Computational Insights into Uranium Complexes Supported by Redox-Active α-Diimine Ligands. *Inorg. Chem.* **2012**, *51*, 2058−2064.
(64) Scalmani, G.; Frisch, M. J. Continuous surface charge polarizable continuum models of solvation. I. General formalism. *J. Chem. Phys.* **2010**, *132*, 114110.
(65) Becke, A. D. Density-functional exchange-energy approximation with correct asymptotic-behavior. *Phys. Rev. A* **1988**, *38*, 3098−3100.
(66) Perdew, J. P. Density-functional approximation for the correlation energy of the inhomogeneous electron gas. *Phys. Rev. B* **1986**, *33*, 8822−8824.
(67) Tao, J. M.; Perdew, J. P.; Staroverov, V. N.; Scuseria, G. E. Climbing the density functional ladder: Nonempirical meta-generalized gradient approximation designed for molecules and solids. *Phys. Rev. Lett.* **2003**, *91*, 146401.
(68) Perdew, J. P.; Burke, K.; Ernzerhof, M. Generalized gradient approximation made simple. *Phys. Rev. Lett.* **1996**, *77*, 3865−3868.
(69) Perdew, J. P.; Burke, K.; Ernzerhof, M. Errata: Generalized gradient approximation made simple. *Phys. Rev. Lett.* **1997**, *78*, 1396−1396.
(70) Lee, C.; Yang, W.; Parr, R. G. Development of the Colle-Salvetti correlation-energy formula into a functional of the electron density. *Phys. Rev. B* **1988**, *37*, 785−789.
(71) Fukui, K. The path of chemical-reactions - The IRC approach. *Acc. Chem. Res.* **1981**, *14*, 363−368.
(72) Hratchian, H. P.; Schlegel, H. B. In *Theory and Applications of Computational Chemistry: The First 40 Years*; Dykstra, C. E., Frenking, G., Kim, K. S., Scuseria, G., Eds.; Elsevier: Amsterdam, 2005; pp 195−249.
(73) Frisch, M. J.; Trucks, G. W.; Schlegel, H. B.; Scuseria, G. E.; Robb, M. A.; Cheeseman, J. R.; Scalmani, G.; Barone, V.; Mennucci, B.; Petersson, G. A.; Nakatsuji, H.; Caricato, M.; Li, X.; Hratchian, H. P.; Izmaylov, A. F.; Bloino, J.; Zheng, G.; Sonnenberg, J. L.; Hada, M.; Ehara, M.; Toyota, K.; Fukuda, R.; Hasegawa, J.; Ishida, M.; Nakajima, T.; Honda, Y.; Kitao, O.; Nakai, H.; Vreven, T.; Montgomery, J. A., Jr.; Peralta, J. E.; Ogliaro, F.; Bearpark, M.; Heyd, J. J.; Brothers, E.; Kudin, K. N.; Staroverov, V. N.; Kobayashi, R.; Normand, J.; Raghavachari, K.; Rendell, A.; Burant, J. C.; Iyengar, S. S.; Tomasi, J.; Cossi, M.; Rega, N.; Millam, J. M.; Klene, M.; Knox, J. E.; Cross, J. B.; Bakken, V.; Adamo, C.; Jaramillo, J.; Gomperts, R.; Stratmann, R. E.; Yazyev, O.; Austin, A. J.; Cammi, R.; Pomelli, C.; Ochterski, J. W.; Martin, R. L.; Morokuma, K.; Zakrzewski, V. G.; Voth, G. A.; Salvador, P.; Dannenberg, J. J.; Dapprich, S.; Daniels, A. D.; Farkas, Ö.; Foresman, J. B.; Ortiz, J. V.; Cioslowski, J.; Fox, D. J. *Gaussian 09*, Revision A.02; Gaussian, Inc.: Wallingford, CT, 2009.
(74) Glendening, E. D.; Reed, A. E.; Carpenter, J. E.; Weinhold, F. *NBO*, Version 3.1; University of Wisconsin: Madison, WI.
(75) Mayer, I. Bond order and valence: Relations to Mulliken's population analysis. *Int. J. Quantum Chem.* **1984**, *26*, 151−154.
(76) Pauling, L. In *Nature of the Chemistry Bond*; Cornell University Press: Ithaca, NY, 1960; pp 88−107.
(77) Allred, A. L. Electronegativity values from thermochemical data. *J. Inorg. Nucl. Chem.* **1961**, *17*, 215−221.
(78) Lide, D. R. *CRC Handbook of Chemistry and Physics: A Ready-Reference Book of Chemical and Physical Data*; CRC Press: London, 2002.